Conductivity Fluctuations of Polycrystalline Ag-Doped YBa$_2$Cu$_3$O$_{7-\delta}$ Superconductor

Paula de Azambuja, Pedro Rodrigues Júnior, Alcione Roberto Jurelo,* and Rosângela Menegotto Costa
Departamento de Física, Universidade Estadual de Ponta Grossa,
Av. Gen. Carlos Cavalcanti 4748, 84.030-000, Ponta Grossa, Paraná, Brazil

Systematic conductivity measurements near T_C in granular Ag-doped YBa$_2$Cu$_3$O$_{7-\delta}$ superconductors are presented. Silver doped YBa$_2$Cu$_3$O$_{7-\delta}$ samples were produced by different routes and characterized by X-ray diffraction, *dc* magnetization and electrical resistivity. The results were analyzed in terms of the temperature derivative of the resistivity and of the logarithmic temperature derivative of the conductivity, that allowed identifying power-law divergences in the conductivity. The results show that the resistive transition proceeds in two stages. In the normal phase, Gaussian and critical fluctuation conductivity regimes were identified. Close to the zero-resistance temperature, a coherence transition related to the connective nature of the granular samples was evidenced. It was not observed significant differences in critical and Gaussian fluctuations between pure and Ag-doped YBa$_2$Cu$_3$O$_{7-\delta}$ polycrystalline samples.

1. INTRODUCTION

Numerous studies have shown that Ag-doping of YBa$_2$Cu$_3$O$_{7-\delta}$ superconductors results in improved superconducting properties in bulk samples [1-5], as for example, the mechanical properties of melt-textured YBCO [3,5]. Also, as Ag fills the intergranular spaces, it improves the electrical properties of the samples, enhancing the critical current density without changing the superconducting transition temperature T_C [6]. On the other hand, silver ions can also be encountered inside the YBCO grains [7]. In addition to its excellent chemical compatibility with YBCO, substitutional Ag produces small modifications in the a and b lattice parameters. Yet, as copper and silver are from the same group of the periodic table, Ag atoms can substitute Cu(1) in the YBCO, and consequently many physical properties can be affected by the presence of microscopic granularity. [8-10].

The aim of this work is to carefully study the resistive transition of pure and Ag-doped YBCO polycrystalline samples. An important point to study is the influence of the Ag ion in the fluctuation regimes, especially in the critical regimes. The silver doped YBCO samples were produced by different routes and characterized by X-ray diffraction, *dc* magnetization and electrical resistivity. More details of material preparation and their general characterization are given in Ref. [11]. The data were analyzed in terms of the temperature derivative of the resistivity ($d\rho/dT$) and also using the logarithmic temperature derivative of the conductivity ($-d\ln(\Delta\sigma)/dT$). The results provide information on the resistive transition and fluctuation conductivity of pure and Ag-doped YBCO samples, and show that the resistive transition proceeds in two steps as shown by the temperature derivative of the resistivity near T_C. The analysis of the conductivity in the normal phase has shown contributions from Gaussian and critical fluctuations. In the regime of near zero resistance state, the occurrence of a coherence transition was evidenced.

2. EXPERIMENTAL DETAILS

A series of samples were prepared by a conventional solid-state reaction using high-purity powders of Y$_2$O$_3$, BaCO$_3$, CuO, Ag$_2$O and metallic Ag. We have prepared four different groups of samples. The group A (labeled by GA) consisted of pure YBCO samples prepared by solid-state reaction technique, using starting materials of Y$_2$O$_3$, BaCO$_3$, and CuO. Appropriate amounts were mixed and calcined in air at 870, 900 and 920 ^{0}C for 24 hours, and then slowly cooled through 700 ^{0}C. Finally, the samples were heated in flowing oxygen at 420 ^{0}C for 24 hours. In group B (GB), a fully oxygenated 1:2:3 compound was first prepared by the usual solid-state reaction method described above. Samples of composition $YBa_2Cu_3O_{7-\delta}/Ag$, with Ag$_2$O 20 wt % were then prepared from Ag$_2$O and 1:2:3 powders. The Ag$_2$O and stoichimetric YBCO powders were well mixed, pressed into pellets and sintered at 920 ^{0}C for 24 hours. The samples were heated in flowing oxygen at 420 ^{0}C for 24 hours.

$$YBa_2Cu_3O_{7-\delta} + 20wt\%Ag_2O \rightarrow YBa_2Cu_3O_{7-\delta}/Ag\,(GB)$$
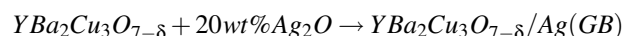
Samples in group C (GC) were prepared with the same chemical formula as in group A, but instead of using the prereacted 1:2:3, we used Y$_2$O$_3$, BaCO$_3$, CuO and Ag$_2$O as precursors.

$$1/2Y_2O_3 + 2BaCO_3 + 3CuO + 20wt\%Ag_2O \rightarrow YBa_2Cu_3O_{7-\delta}/Ag\,(GC)$$
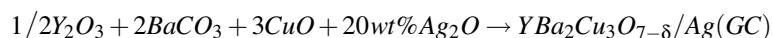
In group D (GD), samples of composition $YBa_2Cu_3O_{7-\delta}/Ag$ with pure Ag (metallic) 20 wt % were prepared from Ag and the prereacted 1:2:3 powders. The Ag and stoichimetric YBCO powders were well mixed, pressed into pellets and sintered at 920 ^{0}C for 24 hours. The samples were heated in

flowing oxygen at 420 ^{0}C for 24 hours.

$$YBa_2Cu_3O_{7-\delta} + 20wt\%Ag \rightarrow YBa_2Cu_3O_{7-\delta}/Ag(GD)$$
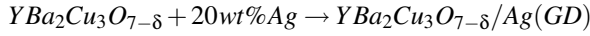
The electrical resistivity as a function of temperature was measured by means of a four-probe AC technique at the frequency of 37 Hz. The measuring current was limited to 100 mA for bar-shaped samples which were approximately 8 x 4 x 3 mm^3. The temperature was determined with an accuracy of 0.01 K by precisely measuring the resistance of a Pt-100 sensor. The X-ray diffraction patterns were collected from 20^0 to 80^0 in the 2θ range with 0.02^0 step and 4 s counting time. The measurements were performed using a Shimadzu X-ray diffractometer with CuK_α radiation and λ = 1.542 Å, and the crystal structure analyses were performed using the GSAS program [12] with the EXPGUI interface [13] and the Le Bail method. The magnetic measurements were obtained by a superconducting quantum interference device MPMS-XL magnetometer from Quantum Design. The critical current density (J_C) was determined by $M - H$ hysteresis loops and using the Bean [14] model from the magnetization curves at 15 K.

3. RESULTS AND DISCUSSION

3.1. Characterization

The X-ray powder diffraction patterns of the pure and Ag-doped YBCO polycrystalline samples are displayed in Figure 1. The patterns almost completely matches the orthorhombic YBCO structure (compared with JCPDS files) and belongs to the YBCO orthorhombic unit cell with symmetry *Pmmm*. Also, all samples are found to be nearly single-phase. For the doped samples we could clearly identify three silver peaks, namely the $Ag(111)$, $Ag(200)$ and $Ag(220)$ reflections, which indicates the presence of silver as a separate (metal) phase [15]. The values of the lattice parameters *a* and *b* are approximately the same for all samples. On the other hand, the lattice parameter *c* decrease from 11.695 (4) Å for pure sample to 11.683 (2) Å for GB, 11.680 (2) Å for GC and to 11.650 (3) Å for GD sample. The change of *c* lattice parameter with Ag addition suggests the presence of silver inside the grains [16]. The obtained lattice parameters are in agreement with published results [8-10].

Fig. 2 shows the temperature dependence of the electrical resistivity of the silver doped YBCO samples GB, GC and GD. The curves are normalized to unity at 95 K. The measured values for ρ $(T = 300K)$ are within the range of the reported values for the YBCO/Ag and all samples exhibit metallic behavior in the normal state. The transition width, ΔT, defined between 5 % and 95 % of the transition height, is approximately 1.5 K for GB, 1 K for GC and 1.2 K for GD. On the other hand, the zero-resistance temperature was approximately $T_{CO} \cong$ 91.5 K for GB, 91.2 K for GC and 91.4 K for GD.

In Fig. 3(a) we show a plot of the derivative $d\rho/dT$ versus temperature for all samples. The maximum of $d\rho/dT$, denoted by T_P, corresponds approximately to the bulk critical temperature [17]. For our samples, T_P is approximately 91.2 K for sample GA, 92.7 K for GB, 91.8 K for GC and
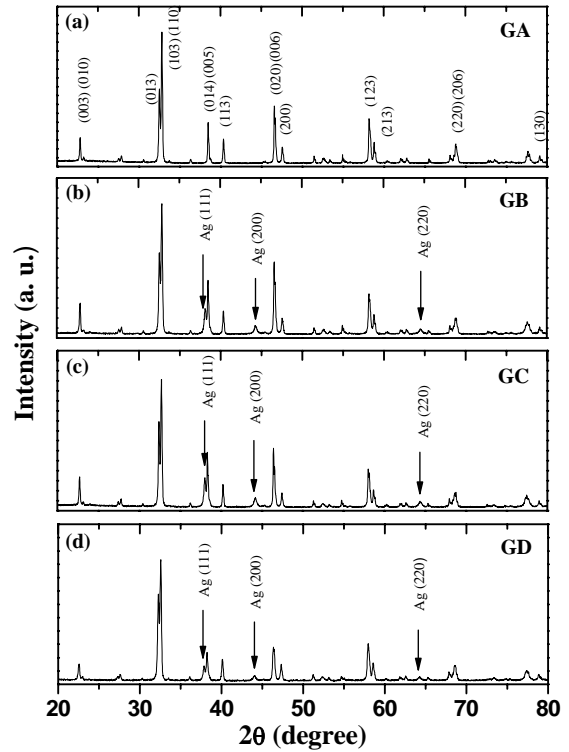

FIG. 1: Representative X-ray diffraction patterns for the pure YBCO (GA) and for the silver doped YBCO samples (GB, GC and GD)
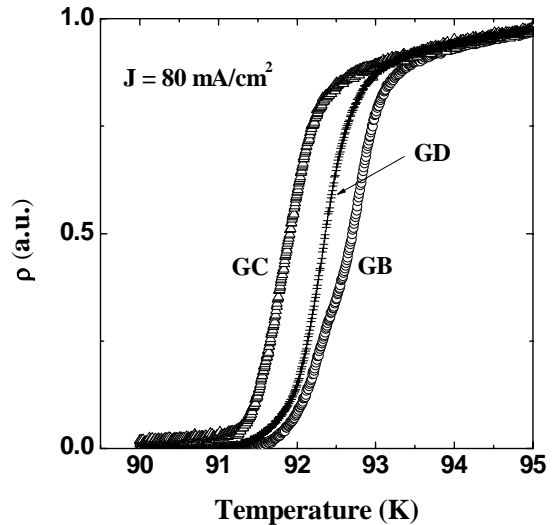

FIG. 2: Temperature dependence of the electrical resistivity for silver doped YBCO samples (GB, GC and GD).

92.3 K for GD, showing that the GB sample has the highest T_P. The same result can be observed in Fig. 2. We could also see that there is an asymmetry in the temperature region below T_P for the pure YBCO sample (inset), suggesting that the sample must have a strong disorder at mesoscopic level [18-19]. From conductivity measurements and fluctuation-induced conductivity analysis, it is possible to separate what is granularity at microscopic and mesoscopic levels [19]. A

small peak or an asymmetry in $d\rho/dT$, at the temperature region below T_P, occurs systematically in polycrystalline samples, indicating that the transition is a two-step process [17]. As the temperature decreases, it is first observed a pairing transition and then a coherence transition. At the pairing transition, the superconductivity stabilizes in homogeneous regions within the grains at a temperature which virtually coincides with the critical temperature of the bulk, T_C. At a lower temperature, T_{CO}, the phase of the order parameter in individual grains becomes long-range ordered. This is the coherence transition, where a long-range superconducting state is achieved through a percolation-like process which controls the activation of weak links between grains. In Fig. 3(b) we show a plot of $d\rho/dT \times T$ in the temperature range where resistance approaches to zero for all samples. To compare the width of the coherence transition among all studied samples we adjusted the temperatures from the T_P value of the GA sample $\left(T_P^{GA}\right)$ calculating $T - \left(T_P - T_P^{GA}\right)$. From the figure 3(b) we can observe that the YBCO/Ag samples have small coherence transition width since T_{CO}, in these samples, are significantly larger.

Critical currents densities J_C for samples GA, GB, GC and GD are shown in Fig. 4. The critical current densities were calculated using the Bean model from the magnetization curves at 15 K. As illustrated in figure, the critical current densities can reach approximately 1450 mA/cm^2 (for samples GA and GD), 2000 mA/cm^2 (GB) and 1650 mA/cm^2 (GC) in $H = 0\,T$. The figure also shows that J_C decreases rapidly with increasing applied magnetic field and that the critical current density (for all applied magnetic field) is significantly higher for sample GB than for other samples.

3.2. Fluctuation Regimes

Thermal fluctuations create Cooper pairs in superconductors above the critical temperature, giving rise to a conductivity excess, also called paraconductivity. We analyze our data supposing that the fluctuation conductivity, $\Delta\sigma$, diverges as a power-law given by

$$\Delta\sigma = A\varepsilon^{-\lambda}, \qquad (1)$$

where $\Delta\sigma = \sigma - \sigma_R$, A is a constant, $\varepsilon = (T - T_C)/T_C$ is the reduced temperature and λ is the critical exponent. σ_R is obtained by linear extrapolation of the resistivity data in the range between 150 K and the room temperature.

To obtain the values for λ and T_C, we numerically determine the logarithmic derivative of $\Delta\sigma$ from experimental data and define

$$\chi_\sigma = -\frac{d}{dT}\ln(\Delta\sigma). \qquad (2)$$

Combining (1) and (2), we obtain

$$\frac{1}{\chi_\sigma} = \frac{1}{\lambda}(T - T_C). \qquad (3)$$

From Eq. (3) is possible to determine simultaneously T_C and λ by plotting χ_σ^{-1} versus T [19].

In Figure 5 we show the resistive transition of GB sample. The measurement was performed with a current density of 800 mA/cm^2. In panel (a) $d\rho/dT$ as a function of
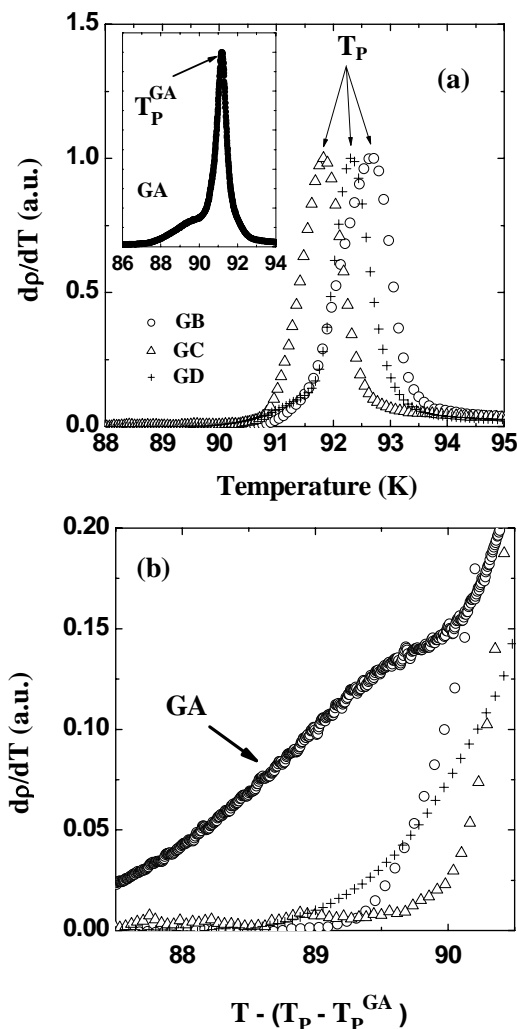

FIG. 3: (a) Plot of $d\rho/dT$ versus temperature ($J = 800$ mA/cm^2) for silver doped YBCO (GB, GC and GD). In the inset it is shown $d\rho/dT$ versus T the pure sample (GA). (b) The plot of $d\rho/dT \times T - \left(T_P - T_P^{GA}\right)$ allows the comparison of the coherence transition's width among all studied samples.

T results is plotted. The zero resistance temperature, T_{C0}, is achieved at approximately 91 K, and we can observe that $T_P \cong 93$ K. Also, we can identify the temperature interval relevant for studying fluctuations in the normal phase (above T_P) and the regime dominated by mesoscopic granularity (close to the $\rho = 0$ state) [19]. In panel (b), the transition is shown as χ_σ^{-1} versus T in the same temperature interval. We can fit χ_σ^{-1} by four power-law regimes, corresponding to four different exponents. These fits are labeled by the indices λ_{cr}, λ_1, λ_2 (all observed above T_P) and s (observed between T_{CO} and T_P). Far from T_P, we can observe a regime dominated by Gaussian fluctuations, labeled by the exponent $\lambda_2 = 0.85 \pm 0.02$. This exponent does not correspond to an integer dimensionality. In this case we supose that the flucutations develop in a space having fractal topology. According Char and Kapitulnik [20], the conductivity exponent should be written as $\lambda = 2 - \frac{\tilde{d}}{2}$ where $\tilde{d}$ is the fractal dimension of the fluctuation network.
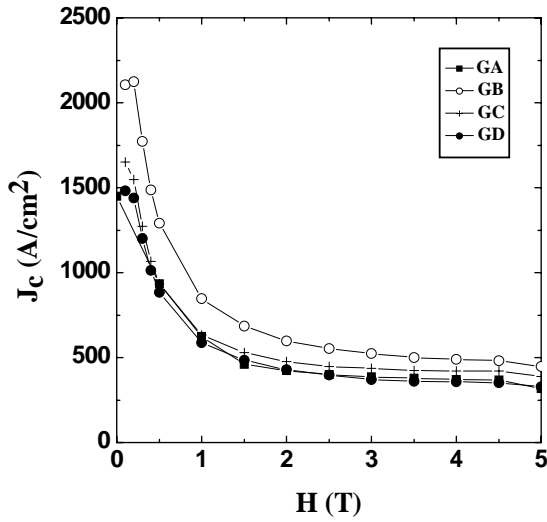
FIG. 4: Critical current densities versus applied magnetic field for the studied samples. The measurements were performed at $T = 15$ K.

Our exponent $\lambda_2 \approx 0.85$ corresponds to a crossover regime between 2D and 3D geometries, with $\tilde{d} \cong 2.3$. Decreasing the temperature, a second Gaussian power-law regime is characterized by the exponent $\lambda_1 = 0.50 \pm 0.03$. As predicted by Aslamazov and Larkin [21], the Gaussian exponents depend on the dimensionality as $\lambda_G = 2 - d/2$, where λ_G is the critical exponent and d is the dimension of the fluctuations system. Then, the exponent $\lambda_1 = 0.50$ is just the predicted one for homogeneous $3D$ fluctuations. In the immediate vicinity above T_P, a crossover occurs to a scaling given by exponent $\lambda_{cr} = 0.31 \pm 0.02$. The critical exponent for fluctuation conductivity is given by

$$\lambda_{cr} = \nu \left(2 + z - d - \eta\right), \qquad (4)$$

where ν is the critical exponent for the coherence length, z is the dynamical exponent, d is the dimensionlaty and η is the exponent for the order-parameter correlation function [22]. The obtained value is consistent with predictions of the $3D - XY$ model, where $\nu = 0.67$ and $\eta = 0.03$ [23]. The dynamics is described by the model E of Hohenberg and Halperin [24], where $z = 1.5$. This regime was also observed in polycrystalline and single-crystal samples [25-27]. Between T_{CO} and T_P, χ_σ^{-1} is well described by a power law regime, given by the equation $\Delta\sigma \propto \left(T - T_{CO}\right)^{-s}$, with $s = 3.2 \pm 0.2$ (inset). This power-law behavior is suggestive of a phase transition phenomenon. For $s \approx 3.0$ exponent, Rosenblatt proposed an interpretation based on a paracoherent-coherent transition of the artificially prepared granular arrays [28,29]. The power-law regime with exponent approximately $s = 3$ was also observed in granular samples of $YBa_2(Cu_{3-x}Zn_x)O_{7-\delta}$ [30], $GdBa_2Cu_3O_{7-\delta}$ [31] and $Bi_{1.6}Pb_{0.4}Sr_2Ca_{n-1}Cu_nO_x$ ($n = 2$ or $n = 3$) [21] near the zero resistance state.

In Fig. 6, we show χ_σ^{-1} as a function of temperature for sample GC. T_P is signaled and the measurement was also performed with a current density of 800 mA/cm^2. Above T_P, we can fit χ_σ^{-1} by three power-law regimes corresponding to different exponents, labeled by the indices λ_{cr}, λ_1 and λ_2. It was
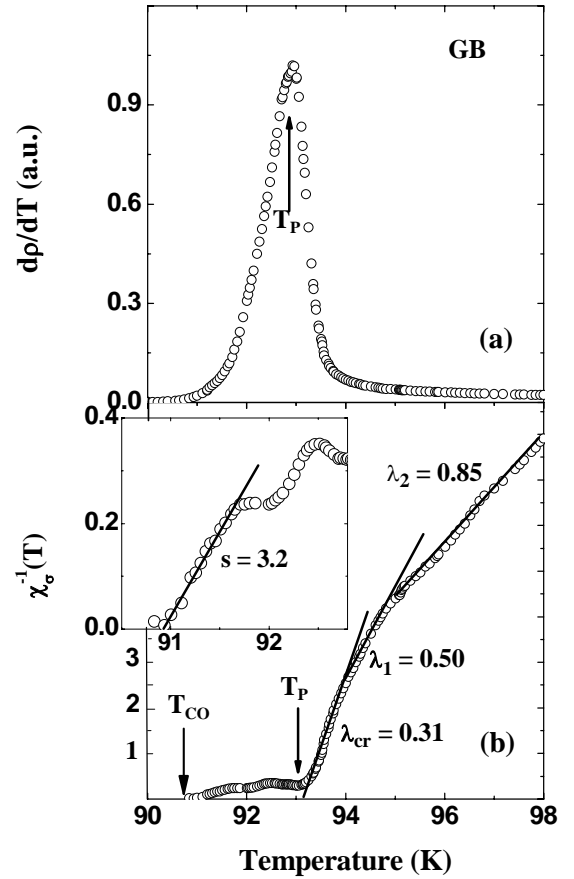

FIG. 5: Representative results of the resistive transition for GB sample. (a) $d\rho/dT$ and (b) χ_σ^{-1} as a function of T. Straight lines are fits to Eq. (3), and the corresponding exponents are given. Current density was 800 mA/cm^2. In the inset of panel (b), an enlarged view of the s regime is shown.

not observed power-law regimes between T_{CO} and T_P. The regimes $\lambda_1 = 0.51 \pm 0.02$ and $\lambda_2 = 1.1 \pm 0.1$ are dominated by Gaussian fluctuations [20,23], corresponding to a homogeneous $3D$ and $2D$ regimes, respectively. Also, closer and above to T_P it is observed a third power-law regime, labeled by the exponent $\lambda_{cr} = 0.31 \pm 0.01$, and that corresponds to genuine critical fluctuations consistent with predictions of the $3D - XY$ model [24].

Figure 7 shows the inverse of the logarithmic derivative of the conductivity, χ_σ^{-1}, as a function of temperature for GD sample ($J = 800$ mA/cm^2). The maximum of $d\rho/dT$ is signaled and can be observed a set of fluctuation regimes labeled by $\lambda_{cr}^{(1)}$, $\lambda_{cr}^{(2)}$, λ_1 (all observed above T_P) and s (observed between T_{CO} and T_P). The exponent $\lambda_1 = 0.55 \pm 0.03$ corresponds to homogeneous $3D$ fluctuations while the exponent $\lambda_{cr}^{(2)} = 0.32 \pm 0.03$ characterizes the asymptotic regime precursor to the pairing transition, and consistent with the $3D - XY$ model [22]. If we analyze χ_σ^{-1} in a temperature range sufficiently close to T_P, a power-law regime with exponent $\lambda_{cr}^{(1)} = 0.21 \pm 0.02$ is observed. This regime, beyond $3D - XY$, was first observed by Costa *et al.* in YBCO single crystal [32]. In Ref. [32] the authors suggested that the
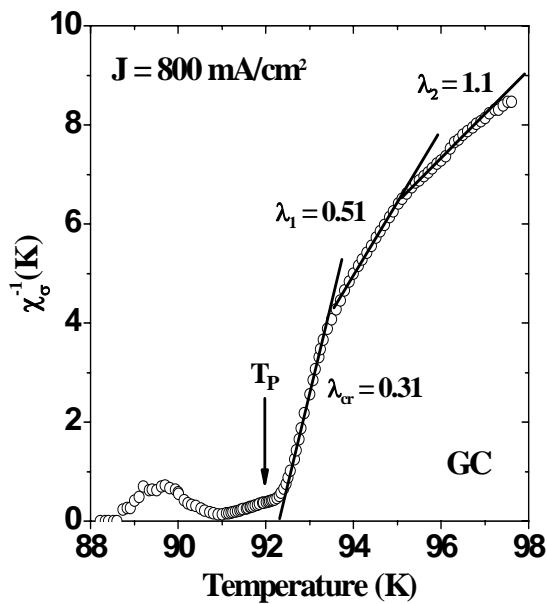
FIG. 6: Plot of the inverse of the logarithmic derivative of the conductivity χ_σ^{-1} as a function of T for GC sample.

$\lambda_{cr}^{(1)}$ regime might be precursor to a weak first-order pairing transition. A first-order transition occurs when the absolute minimum of the Ginzburg-Lanudau free-energy switches discontinuously from the high temperature position, $|\psi| = 0$, to the one with nonzero $|\psi|$. One can expect that above but in close vicinity to T_C, the system is allowed to fluctuate between the two free-energy minima because of the low height of the barrier that separates them. This could affect the system dynamics, modifying the effective value of z. The value $\lambda_{cr}^{(1)} \cong 0.21$ may be reproduced if $z \cong 1.34$ in Eq. (4) [33]. It is not clear why only the GD sample presents a beyond $3D - XY$ regime. More studies are necessary to clarify this point. Between T_{CO} and T_P the variation of χ_σ^{-1} as a function of temperature is again described by a power-law regime given by the exponent $s = 3.3 \pm 0.1$, and that corresponds to a phase transition from a paracoherent to a coherent state of the granular array [18,30].

From the results we observe that Ag doping does not modify significantly the value of the critical exponents neither above T_P (related with the pairing transition) neither below T_P (related with the coherence transition). On the other hand, we clearly note that silver addition decreases the coherence transition width when compared with the pure sample. Among all the studied samples, the GB sample presented the highest T_P, the highest critical current density and the smallest coherence transition width. When mixed to the YBCO, silver is mainly incorporated in the intergrain regions providing a better grain coupling. In our view, better grain coupling in the sample

GB is due to the fact that the grains in the Ag_2O are smaller than the grains in the metallic Ag. Consequently, a more efficient intergrain Ag diffusion occurs in route B. In route C, probably, a small quantity of silver atoms penetrate inside the grains. This effect enhances the intragrain granular character of sample GC.
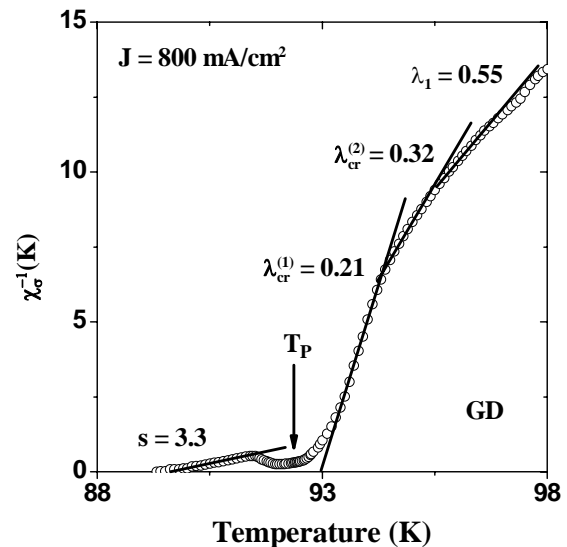

FIG. 7: Plot of the inverse of the logarithmic derivative of the conductivity χ_σ^{-1} as a function of T for GD sample.

4. CONCLUSION

In conclusion, we have studied fluctuations on the electrical conductivity in polycrystalline Ag-doped $YBa_2Cu_3O_{7-\delta}$ superconductor. The Ag-doped $YBa_2Cu_3O_{7-\delta}$ samples were produced by different routes and characterized by X-ray diffraction, *dc* magnetization and electrical resistivity. From the temperature derivative of the resistivity, the results revealed the occurrence of a two-stage intragranular-intergranular transition. From of the logarithmic temperature derivative of the conductivity we could clearly observe above T_C the presence of Gaussian and critical regimes while in the regime of near zero resistance state, the occurrence of a coherence transition was evidenced. The Ag doping does not modify expressively the value of the critical exponents, but causes a significant decrease of the coherence transition width when compared with the pure sample.

[1] E. Mogilko, Y. Schlesinger, Supercond. Sci. Technol. 10 (1997) 134.

[2] J. Joo, J.G. Kim, W. Nah, Supercond. Sci. Technol. 11 (1998) 1285.

[3] G. Krabbes, G. Fuchs, P. Schtzle, S. Gruss, J.W. Park, F. Hardinghaus, R. Hayn, S.L. Dreschler, Physica C 341-348 (2000)

2289.

[4] E. Mendonza, T. Puig, E. Varesi, A.E. Carrillo, J. Plain, X. Obradors, Physica C 334 (2001) 7.

[5] D. Behera, N C Mishra, Supercond. Sci. Technol. 15 (2002) 72.

[6] A.P. Li, Q.N. Ni, Q.P. Kong, Phys. Status Solidi a 27 (1991) 187.

[7] C.R. Taylor, C. Greaves, Physica C 235-240 (1994) 853.

[8] D. Cahen, Z. Moisi, M. Schwartz, Mater. Res. Bull. 22 (1987) 1581.

[9] A.K. Gangopadhyay, T.O. Mason, Physica C 178 (1991) 64.

[10] J. Joo, J.P. Singh, R.B. Poeppel, A.K. Gangopaddhyay, T.O. Mason, J. Appl. Phys. 71 (1992) 2351.

[11] Submitted paper "Effects of Ag Addition on Some Physical Properties of Granular $YBa_2Cu_3O_{7-\delta}$ Superconductor" in the Brazilian Journal of Physics.

[12] A.C. Larson, R.B. Von Dreele, GSAS, Los Alamos National Laboratory (2004) Report LAUR 86-748.

[13] B.H. Toby, J. Appl. Cryst. 34 (2001) 210.

[14] C. P. Bean, Rev. Mod. Phys. 36 (1964) 31.

[15] H. Salamati, A.A. Babaei-Brojeny, M. Safa, Supercond. Sci. Technol. 14 (2001) 816.

[16] O. Grr, C. Terzioglu, A Varilici, M Altunbas, Supercond. Sci. Technol. 18 (2005) 1.233.

[17] A.R. Jurelo, I.A. Castillo, J. Roa-Rojas, L.M. Ferreira, L. Ghivelder, P. Pureur, P. Rodrigues Jr., Physica C 311 (1999) 133.

[18] P. Pureur, R. Menegotto Costa, P. Rodrigues Jr., J. Schaf, J.V. Kunzler, Phys. Rev. B 47 (1993) 11.420.

[19] A.R. Jurelo, J.V. Kunzler, J. Schaf, P. Pureur, J. Rosenblatt, Phys. Rev. B 56 (1997) 14.815.

[20] K. Char and A. Kapitulnik, Z. Phys. B 72 (1988) 256.

[21] L.G. Aslamazov, A.I. Larkin, Fiz. Tverd. Tela 10 (1968) 1104.

[22] B. Oh, K. Char, A.D. Kent, M. Naito, M.R. Beasley, T.H. Geballe, R.H. Hammon, A. Kapitulnik, J. M. Graybeal, Phys. Rev. B 37 (1988) 7861.

[23] J.C. Le Guillou, J. Zinn-Justin, Phys. Rev. B 21 (1980) 3976.

[24] P.C. Hohenberg, B.I. Halperin, Rev. Mod. Phys. 49 (1977) 435.

[25] F.M. Barros, F.W. Fabris, P. Pureur, J. Schaf, V.N. Vieira, A.R. Jurelo, M.P. Canto, Phys. Rev. B 73 (2006) 94.516.

[26] J. Roa-Rojas, A.R. Jurelo, R. Menegotto Costa, L.M. Ferreira, P. Pureur, M.T.D. Orlando, P. Prieto, G. Nieva, Physica C 341-348 (2000) 1911.

[27] R. Menegotto Costa, P. Pureur, L. Ghivelder, J.A. Camp, I. Rasines, Phys. Rev. B 56 (1997) 10.836.

[28] J. Rosenblatt, A. Raboutou, P. Peyral, C. Lebeau, Rev. Phys. Appl. 25 (1990) 73.

[29] J. Rosenblatt, in Percolation, Localization and Superconductivity, Vol. 109 of NATO Advanced Study Institute, Series B-Physics, edited by A. M. Goldman and S. A. Wolf (Plenum, New York, 1984), p. 431.

[30] R. Menegotto Costa, L.M. Ferreira, V.N. Vieira, P. Pureur, J. Schaf, Eur. Phys. J. B 58 (2007) 107.

[31] J. Roa-Rojas, R. Menegotto Costa, P. Pureur, P. Prieto, Phys. Rev. B 61 (2000) 12.457.

[32] R. Menegotto Costa, P. Pureur, M. Gusmo, S. Senoussi, K. Behnia, Solid State Communications 113 (2000) 23.

[33] R. Menegotto Costa, P. Pureur, M. Gusmo, S. Senoussi, K. Behnia, Phys. Rev. B 64 (2001) 214513.